

Dipole polarizability of the pyrazabole molecule in solution[†]

Ysaías J. Alvarado,^{1*} Humberto Soscún,² Wendy Velazco,¹ Paola H. Labarca,¹ Nestor Cubillan¹ and Javier Hernández²

¹Laboratorio de Electrónica Molecular, Departamento de Química, Facultad Experimental de Ciencias, La Universidad del Zulia, Ap. 526, Grano de Oro, Módulo No. 2, Maracaibo, Venezuela

²Laboratorio de Química Inorgánica Teórica, Departamento de Química, Facultad Experimental de Ciencias, La Universidad del Zulia, Ap. 526, Grano de Oro, Módulo No. 2, Maracaibo, Venezuela

Received 19 March 2002; revised 2 July 2002; accepted 5 July 2002

ABSTRACT: The dynamic and static dipole polarizabilities of pyrazabole (PYRZ) were investigated using a refractometric method and theoretical calculations. The experimental properties were studied within the Singer–Garito and Proutiere and co-workers' approaches for dilute cyclohexane, THF and CH₃CN solutions. These methodologies were appropriate to quantify the electronic polarizability and electric deformability of pyrazabole in the optical regime. The static dipole polarizabilities of pyrazabole were obtained from extrapolation to zero frequency of the corresponding dispersion Cauchy-type curves, which gave a monotonic increasing in function of the squared frequency. The differences between these curves were analyzed as a function of the solvent effects. Additionally, a comparative study with pyrazole was carried out. The results indicated that both the static and dynamic electronic polarizability of pyrazabole are determined from the linear optical response of the pyrazole ring. In fact, the polarizability of the two pyrazole rings is approximately 80% of the overall value for pyrazabole. The theoretical static properties were evaluated by using *ab initio* (Hartree–Fock) and DFT (B3LYP) methods with the 6–31+G(d,p) and 6–311++G(3d,3p) basis sets. The calculations were performed with fully optimized geometries. The B3LYP average static electronic polarizability value of pyrazabole is 1.877×10^{-23} esu, and the differences from the experimental static values are within –1.2 to 8.5%. These variations are mainly due to the solvent effects. Copyright © 2002 John Wiley & Sons, Ltd.

KEYWORDS: pyrazabole; dipole polarizability

INTRODUCTION

Pyrazaboles compounds are boron–nitrogen heterocycles in which two pyrazole molecules and two BX₂ (X = H, Cl, Br) fragments are arranged in three fused rings. These compounds, which exhibit remarkable stability, were first reported by Trofimenko simultaneously with poly(pyrazolyl)borate ions.¹ Owing to their electronic and geometric features, polypyrazol-1-ylborate anions have extensive uses as ligands in coordination, bioinorganic and organometallic chemistry.² Furthermore, transition metal complexes containing polypyrazol-1-ylborate ligands have been shown to exhibit exceptional electronic and non-linear optic properties.³ From the structural point

of view, x-ray diffraction studies of the molecular structure of pyrazaboles have shown that these tricyclic systems can adopt planar, boat or chair conformations in the B₂N₄ rings.⁴ Additionally, the thermodynamic properties in alcoholic solutions of some pyrazaboles, including the simplest pyrazabole (PYRZ) (Fig. 1) have been reported.⁵ Despite the importance of these properties and the existence of many derivatives with both boron centers and substituted pyrazolyl rings, little attention has been given to pyrazabole compounds.

Recent reports of chemical behavior of ansa-ferrocene complexes with pyrazabole bridges in solution suggest that pyrazabole compounds are highly polarizable and have exceptional electronic donor and acceptor properties, thereby offering the possibility of influencing the electronic properties of organometallic compounds for specific applications.⁶ In addition, Barbera and Giménez have shown the potential of the pyrazabole ring to generate molecules with liquid crystal properties.⁷

We are currently interested in the determination and prediction of the electronic and optical properties of conjugate heterocyclic molecules and their comparison with available experimental data.⁸ In this work, we extended these studies to the experimental determination of the dipole polarizability of the pyrazabole (PYRZ)

*Correspondence to: Y. Alvarado, Laboratorio de Electrónica Molecular, Departamento de Química, Facultad Experimental de Ciencias, La Universidad de Zulia, Ap. 526, Grano de Oro, Módulo No. 2, Maracaibo, Venezuela.

E-mail: yalvarado@hotmail.com

[†]Presented in part at the Sixth Latin American Conference on Physical Organic Chemistry (CLAQO-6), held at Isla Margarita, Venezuela, during December 2001.

Contract/grant sponsor: CONICIT; Contract/grant number: S1-95001617; Contract/grant number: PG G-97000593.

Contract/grant sponsor: CONICIT/CONIPET; Contract/grant number: 58 97003734.

Contract/grant sponsor: CONDES/LUZ.

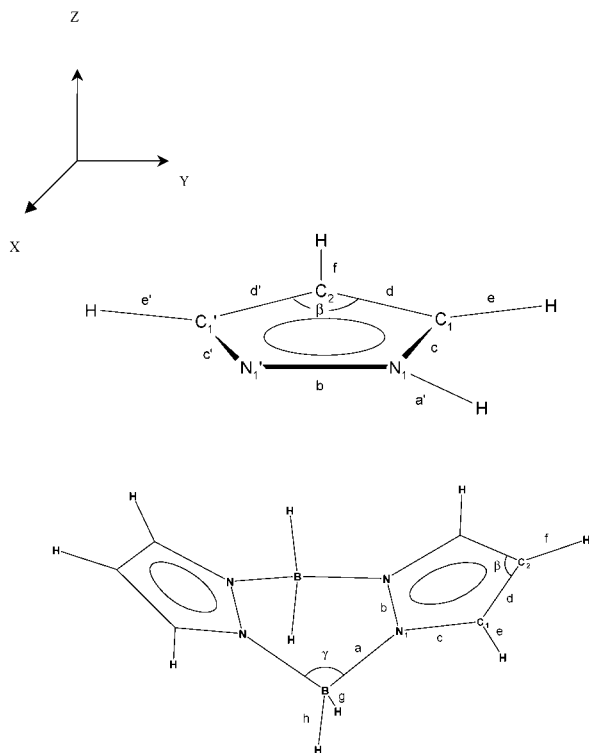


Figure 1. Molecular geometries and axis references for the pyrazole and pyrazobole molecules

molecule and the evaluation of solvent effects on this electronic property by using cyclohexane, THF and CH_3CN . Theoretical calculations were performed for this molecule in the static regime with DFT techniques and extended basis sets as performed for the dibenzothio-*phene* molecule.⁸ Additional measurements and calculations of the polarizability were performed on the pyrazole (PYR) molecule to account for the contribution of the pyrazole ring to the overall polarizability of PYRZ.

THEORY

Electric dipole polarizability

The molecular dipole polarizability α is the linear response of a molecular electronic distribution to the action of an external electric field \mathfrak{E} . Such an external field induces charge rearrangements that are reflected in changes in the permanent molecular dipole moment μ_e according to the equation^{9a}

$$\mu_e(\mathfrak{E}) = \mu_e(\mathfrak{E} = 0) + \alpha\mathfrak{E} + (1/2!)\beta\mathfrak{E}^2 + (1/3!)\gamma\mathfrak{E}_i\mathfrak{E}_j\mathfrak{E}_k\mathfrak{E}_l + \dots \quad (1)$$

where $\mu_e(\mathfrak{E} = 0)$ is the permanent dipole moment in the absence of a field. The terms of higher order are the first and second hyperpolarizabilities, respectively. Similarly,

a Taylor expansion for the energy E of the system has been defined in terms of the dipole polarizabilities and the field \mathfrak{E} as

$$E(\mathfrak{E}) = E(0) - \mu_i\mathfrak{E}_i - (1/2)\alpha_{ij}\mathfrak{E}_i\mathfrak{E}_j - (1/6)\beta_{ijk}\mathfrak{E}_i\mathfrak{E}_j\mathfrak{E}_k - (1/24)\gamma_{ijkl}\mathfrak{E}_i\mathfrak{E}_j\mathfrak{E}_k\mathfrak{E}_l + \dots \quad (2)$$

where $E(0)$ is the unperturbed energy.^{9b}

The experimental determination of a molecular polarizability is far from straightforward, especially if the molecule has little or no symmetry. For a molecule with symmetry, the axes of the polarizability tensor correspond to the symmetry axes. Otherwise, the principal axes have to be determined by diagonalization of the polarizability matrix. The principal axes are usually referred to as a , b and c .^{9b} We will adopt the convention

$$\alpha_{aa} < \alpha_{bb} < \alpha_{cc} \quad (3)$$

where the α_{ii} are the eigenvalues of the polarizability matrix. The quantities of experimental interest are the average polarizability

$$\alpha_{\text{ave}} = \langle \alpha \rangle = 1/3(\alpha_{aa} + \alpha_{bb} + \alpha_{cc}) \quad (4)$$

and the polarizability anisotropy

$$\Delta\alpha = \{(1/2)[(\alpha_{aa} - \alpha_{bb})^2 + (\alpha_{aa} - \alpha_{cc})^2 + (\alpha_{bb} - \alpha_{cc})^2]\}^{1/2} \quad (5)$$

The average polarizability can be determined experimentally from the refractive index η of a gas according to the equation

$$\eta = 1 + \frac{2\pi\langle \alpha \rangle \sigma}{k_B T} \quad (6)$$

where σ is the pressure, k_B the Boltzmann constant and T the thermodynamic temperature. Equation (6) was derived with the assumption that the individual molecules do not interact with each other. However, in the condensed phase molecular interactions should be considered. In this case, each molecule is polarized by the external field and the field due to the surrounding molecules. The resultant field, referred as local field F , is expressed in terms of the dielectric polarization P as

$$F = E + 4\pi LP \quad (7)$$

where L is the dimensionless Lorentz factor that depends on the structure of the phase, and is a tensor the three principal components of which have the value of 1/3 for cubic and isotropic phases, giving the Lorentz local field

$$F = E + \frac{4\pi}{3}P \quad (8)$$

From this equation can be derived the Lorentz–Lorentz

equation:

$$\frac{\eta^2 - 1}{\eta^2 + 2} = \frac{4\pi N \langle \alpha \rangle}{3V} \quad (9)$$

which gives an expression for the average molecular polarizability $\langle \alpha \rangle$, and N is the number of molecules in volume V . For molecules with a permanent dipole moment μ_e , it is necessary to take account of the orientational polarization. The resulting Debye equation:

$$\frac{M \varepsilon_r - 1}{\rho \varepsilon_r + 2} = \frac{4\pi N_A}{3} \left(\langle \alpha \rangle + \frac{\mu_e^2}{3k_B T} \right) \quad (10)$$

permits the average polarizabilities and dipole moment to be determined from measurements of the relative permittivity ε_r and the density ρ as a function of the temperature T .^{9c} M is the molar mass and N_A is Avogadro's number. The application regime of this equation is only for pure compounds. Experimentally, $\langle \alpha \rangle$ is determined at electric fields that depend of the frequency and the dynamic property is obtained. In the regime of optical frequencies, Eqn. (10) is converted to the Eqn. (9). From Eqn. (9) and for binary mixtures, such as solvent and solute, the equation of Singer and Garito can be derived.^{10a}

$$\begin{aligned} \frac{4\pi}{3} N_A \alpha_{2(v)}^e &= \frac{3M_2}{\rho_1 [\eta_1^2(v) + 2]^2} \left(\frac{\partial \eta^2(v)}{\partial w} \right)_0 \\ &+ M_2 \left[\frac{1}{\rho_1} + \left(\frac{\partial V}{\partial w} \right)_0 \right] \left[\frac{\eta_1^2(v) - 1}{\eta_1^2(v) + 2} \right] \end{aligned} \quad (11)$$

where w is the weight fraction of solute, $\eta_{(v)}$ and $\eta_{1(v)}$ are the refractive indices of solution and solvent at optical frequency ν , respectively, ρ_1 is the density of the solvent, N_A is Avogadro's number, M_2 is the molecular weight of the solute, V is the inverse of the density of solution or specific volume of solution and $\alpha_{2(v)}^e$ is the average of the molecular electronic dynamic polarizability of the solute. Proutière and co-workers proposed an alternative equation for the measurement of refraction in binary solutions using the Lorentz–Lorenz local field [Eqn. (8)].¹¹ The resulting equation is

$$\alpha_{2(v)}^e = \frac{M_2}{M_1} \alpha_1^e(v) \left\{ 1 + \left[\frac{\partial f_r(v)}{\partial w} \right]_{w \rightarrow 0} \right\} \quad (12)$$

where $\alpha_1^e(v)$ is the dynamic mean polarizability of the solvent and the factor f_r is

$$f_r = \rho_1 V \left[\frac{\eta_{(v)} - 1}{\eta_{(v)} + 2} \right] \left[\frac{\eta_{1(v)} + 2}{\eta_{1(v)} - 1} \right] \quad (13)$$

These equations assume that the solute and solvent do not interact and therefore the different molecular polariza-

tions are additive. To obtain the static mean molecular electronic polarizability, the $\langle \alpha \rangle$ dynamic property of either Eqn. (11) or (12) is treated as a frequency-dependent quantity and calculated at different wavelengths. The long-wavelength limit is obtained from an extrapolation to zero frequency of the plot between the dynamic mean polarizability $\alpha_{2(v)}^e$ versus the frequency ν . This relationship is referred as the Cauchy-type dispersion curve and gives the behavior of the dispersion of the polarizability in terms of the frequency of the field. This curve allows for the extrapolation of only the electronic part of this property, the limit value of which corresponds to the static dipole polarizability. Contributions from infrared-active modes (vibrational polarizability) are not considered here.^{8,10bc,12}

EXPERIMENTAL

The average electronic polarizability dispersion curves of the studied compounds were determined experimentally by using refractometric techniques, where the refractive index η of both the solvent and solutions were measured with Bellingham + Stanley 60/LR and 60/LR high-resolution Abbe refractometers with a CCD camera at $20 \pm 0.1^\circ\text{C}$. Sodium, mercury and cadmium spectral lamps were employed in the wavelength range 435.8–643.8 nm. The density ρ was determined by measuring the period of oscillation of a vibrating sample cell with a sample volume of 1 ml on an Anton Paar DMA-5000 densitometer. The values of the refractive index at optical frequency ν and density obtained in this work for each solvent were found to agree satisfactorily with the values reported previously in the literature.^{8,12,13}

Pyrazole (PYR) (99%) was purchased from Merck and was used without further purification. Pyrazabole (PYRZ) (97%) was purchased from Aldrich and recrystallized from anhydrous methanol. The solvents were rigorously dried and fractionally distilled by standard methods and stored over molecular sieves. A series of solutions of PYR and PYRZ in various solvents were prepared. Their UV–visible absorbance spectra were obtained on a Shimadzu Model UV-1201 spectrophotometer. A 1-cm quartz cuvette was used as the sample cell. The weight-fraction concentration range used was 1.798×10^{-3} – 2.041×10^{-2} in all cases. Excellent linear relationships were found for the specific volumes, the function f_r and the square of the refractive indices of the solutions against their weight fractions w_2 at each frequency of the applied electric field. The reproducibility for the various slopes of the concentration dependence for these data was very high and the uncertainties in the dynamic mean electronic polarizabilities obtained in this work were between 0.93 and 1.95%.

COMPUTATIONAL DETAILS

The molecular geometries of pyrazole and pyrazabole, subject to C_s and C_{2v} symmetry restrictions, respectively, were fully optimized by using gradient techniques with the Hartree–Fock (HF) SCF MO and density functional theory (DFT) using the B3LYP method¹⁴ and the 6–31+G(d,p) basis set.¹⁵ Analytical and direct coupled perturbed Hartree–Fock (CPHF)¹⁶ and numeric B3LYP methods were employed to calculate the static electronic dipole polarizability α with the extended basis sets, containing sp diffuse functions plus sets of d and p polarized functions such as 6–31+G(d,p) and 6–311+G(3d,3p).¹⁷ The good performance of these atomic functions for polarizability calculations of conjugated molecules has been pointed out.^{8,12} It is important to note that the B3LYP DFT functional is able to account accurately for the exchange and electron correlation effects in the static dipole polarizability.^{8,12} For the case of pyrazabole, calculations with the Sadlej basis set were additionally performed.¹⁸ The dynamic polarizability was evaluated analytically by using the time-dependent Hartree–Fock (TDHF) method.¹⁹

All calculations were carried out using the Gaussian 98²⁰ quantum chemistry package in an Silicon Graphics Origin 2000 workstation.

RESULTS AND DISCUSSION

Polarizability of pyrazabole

Experimental determination. No estimates for the molecular dipole polarizability of PYRZ have been reported so far. Here we report refractometric measurements for the dispersion of the dipole polarizability of PYRZ using the limit relationships of Singer and Garito^{10a} [see Eqn. (11)] and Proutière and co-workers¹¹ [see Eqn. (12)]. From these results, the static value of this property was obtained. The performance of this methodology has been reported elsewhere by other authors and ourselves.^{8,12,21} Prior to the refractometric measure-

ments, the UV–visible spectrum of PYRZ was measured in the region 200–600 nm to explore the adsorption of this compound. Was found that the lower wavelength Adsorption for this molecule is 280 nm. Additionally, we also studied the molecular interactions in solution taking into account the concentration and solvent effects on the electronic spectra. The solvents used were CH₃CN, THF, cyclohexane and CCl₄. It was found that for each solvent the bandshape of the PYRZ Adsorption does not change with the solute concentration. This suggests that pyrazabole is not able to form stable complexes with the solvents employed. These findings are in agreement with previous observations with polar solvents such as alcohols.⁵ Based on these results, we carried out a study of the dispersion of the dipole polarizability of pyrazabole in the off-resonance region in solution.

The frequency-dependent experimental results of the relevant terms of Eqns (11) and (12) in each solvent are reported in Tables 1 and 2, respectively, and the corresponding Cauchy-type dispersion curves of the dipole polarizability of PYRZ dissolved in tetrahydrofuran (THF), cyclohexane (C₆H₁₂) and acetonitrile (ACN) are shown in Figs 2 and 3.

The dynamic results of the dipole polarizability obtained with Eqn. (11) show how this property increases monotonically with the frequency ν , giving a normal dispersion behavior for the electronic polarizability of pyrazabole in all solvents (see Fig. 2). From this relationship, the extrapolation to zero frequency gives values of 1.792×10^{-23} , 1.827×10^{-23} and 1.730×10^{-23} esu for the static dipole polarizability of pyrazabole in solutions of C₆H₁₂, THF and ACN, respectively (see Table 2 and Fig. 2). The uncertainty of these values, calculated from an analysis of random propagation errors, is about 1.95%.^{8,10b}

Analysis of Table 2 and Fig. 2 shows that the values of the dynamic polarizabilities of pyrazabole are slightly affected by THF and C₆H₁₂ solvents. In fact, the values of the dynamic polarizability of pyrazabole in solution of THF are only 1.5% higher than our experimental results in C₆H₁₂. This difference lies within the experimental

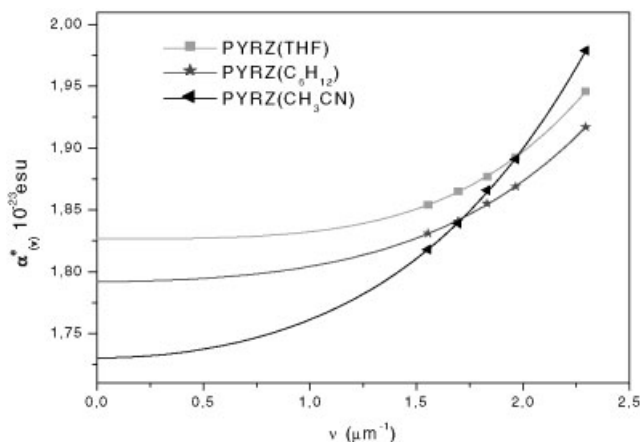
Table 1. Refraction and density measurement values with Eqns (11) and (12) for PYRZ in binary solutions

ν (μm^{-1})	$\left[\frac{\partial \eta_{(\nu)}^2}{\partial w}\right]_{w \rightarrow 0}^a$			$\left[\frac{\partial f_{r(\nu)}}{\partial w}\right]_{w \rightarrow 0}^a$		
	C ₆ H ₁₂ ^b	CH ₃ CN ^c	THF ^d	C ₆ H ₁₂	CH ₃ CN	THF
2.294631	0.2455	0.4391	0.4039	−0.1023	0.1265	0.0854
1.966182	0.2251	0.3926	0.3729	−0.1122	0.0909	0.0675
1.831166	0.2194	0.3800	0.3641	−0.1149	0.0853	0.0627
1.696065	0.2135	0.3657	0.3582	−0.1181	0.0693	0.0598
1.553277	0.2103	0.3551	0.3535	−0.1196	0.0613	0.0580

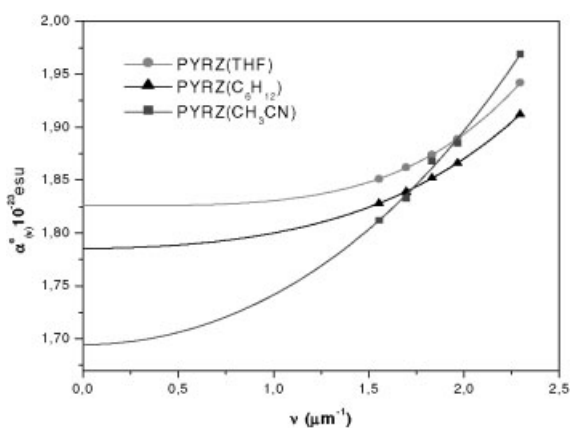
^a $T = 20 \pm 0.1^\circ\text{C}$; $\left(\frac{\partial \nu}{\partial w}\right)_{w \rightarrow 0}^{a,b} = -0.347 \pm 0.003$; $\left(\frac{\partial \nu}{\partial w}\right)_{w \rightarrow 0}^{a,c} = -0.364 \pm 0.002$; $\left(\frac{\partial \nu}{\partial w}\right)_{w \rightarrow 0}^{a,d} = -0.240 \pm 0.005$.

Table 2. Results of dipole polarizability of PYRZ determined from Eqns (11) and (12) in binary solutions

ν (μm^{-1})	$\alpha_2^e \nu (10^{-23} \text{ esu})^a$			$\alpha_2^e \nu (10^{-23} \text{ esu})^b$		
	C_6H_{12}	THF	CH_3CN	C_6H_{12}	THF	CH_3CN
2.294631	1.917	1.946	1.979	1.912	1.942	1.969
1.966182	1.869	1.893	1.891	1.866	1.889	1.885
1.831166	1.855	1.877	1.866	1.852	1.874	1.868
1.696065	1.841	1.865	1.839	1.839	1.862	1.833
1.553277	1.831	1.854	1.818	1.828	1.851	1.812
0.000000	1.792	1.826	1.730	1.785	1.826	1.695

^a Equation (11) and parameters of Table 1.^b Equation (12) and parameters of Table 1.**Figure 2.** Dispersion curves of the mean dipole polarizability of PYRZ obtained with Eqn. (11) in solutions of CH_3CN , C_6H_{12} and THF

error. Moreover, the total electric deformability seen as the variation of polarizability at 435.8 nm ($1.966182 \mu\text{m}^{-1}$) with respect to the static value for pyrazabole is 6.98 and 6.51% in THF and C_6H_{12} , respectively. These results indicate that the electronic

**Figure 3.** Dispersion curves of the mean dipole polarizability of PYRZ obtained with Eqn. (12) in solutions of CH_3CN , C_6H_{12} and THF

properties of pyrazabole are little affected in these aprotic solvents. In CH_3CN solution, a significant change in the polarizability dispersion curve of PYRZ is observed, and the magnitude of the electric deformability of pyrazabole is about of 14.4%. This value higher than those observed in THF and C_6H_{12} (see Fig. 2). This enhanced electronic deformability of PYRZ observed in acetonitrile can be attributed to an important contribution of electric charge separation due to the high polarity of the solvent and a coupled effect with the frequency of the electric field can be seen in Fig. 2. In fact, pyrazabole is highly polarizable at high frequencies of the electric field, whereas it is much less polarizable at lower frequencies, where a crossing between the dispersion curve with ACN and the corresponding curves with THF and C_6H_{12} occurs (see Fig. 2). It is important to note that for the points located after this intersection in the Cauchy curves of Fig. 2, a linear relationship there exists between the dynamic $\langle \alpha_2^e \rangle$ of PYRZ and the permanent dipole moments of the solvents. This correlation it is improved at higher frequencies. For example, at a frequency of $2.294631 \mu\text{m}^{-1}$ the value of the correlation coefficient r^2 is 0.998. This means that at this frequency, the dynamic effects on the $\langle \alpha \rangle$ of PYRZ are dominated by the polarity of the solvents. In contrast, for the region of lower frequencies, the static polarizability of PYRZ in ACN is 5.6% lower than in the other solvents (see Table 2), and no relationship exists with either the dipole moment of the solvents or other important solvent parameters. The results show that in the static regime, the $\langle \alpha \rangle$ of PYRZ is higher in the solvent with lower polarity (cyclohexane) and is lower in the solvent with higher polarity (ACN). Further studies on these findings are being performed in order to give a comprehensive explanation of these observations.

In Table 2 are shown the values of the dynamic and static dipole polarizability of pyrazabole obtained with the equation of Proutière and co-workers. These results are very close to those obtained with Eqn. (11) and indicate that this methodology is also appropriate for the determination of the dynamic polarizability of pyrazabole in solution. Thus, the dispersion of the polarizability curves obtained for Eqns (11) and (12) is similar and the

Table 3. Refraction and density measurement values deduced from Eqns (11) and (12) for PYR in binary solutions

ν (μm^{-1})	$\left[\frac{\partial n_{\nu}^2}{\partial w}\right]_{w \rightarrow 0}^a$		$\left[\frac{\partial f_{\nu}(v)}{\partial w}\right]_{w \rightarrow 0}^a$	
	THF ^b	CH ₃ CN ^c	THF	CH ₃ CN
2.294631	0.3530	0.3928	0.0400	0.0942
1.966182	0.3082	0.3651	0.0081	0.0716
1.831166	0.2919	0.3569	-0.0001	0.0656
1.696065	0.2795	0.3493	-0.0063	0.0598
1.553277	0.2678	0.3431	-0.0159	0.0561

^a $T = 20 \pm 0.1^\circ\text{C}$;

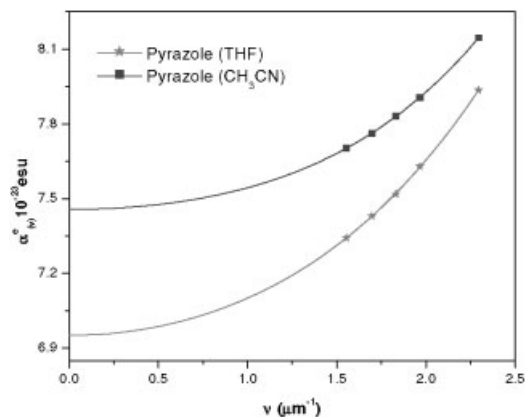
$$\left(\frac{\partial \nu}{\partial w}\right)_{w \rightarrow 0}^{a,b} = -0.249 \pm 0.004; \left(\frac{\partial \nu}{\partial w}\right)_{w \rightarrow 0}^{a,c} = -0.357 \pm 0.002.$$

quality of the fitting of the dynamic mean polarizability of pyrazole values with the frequency of the electric field in the Cauchy-type dispersion curve is of the same significance as that obtained with Eqn. (11) for PYRZ in THF and cyclohexane solutions. This correlation is less satisfactory for ACN solvent, however. The results in Table 2 show that both methodologies [Eqns (11) and (12)] are useful for accurate determination of the average electronic polarizability of molecules in solutions. With Eqn. (11) the behavior of the dynamic $\langle\alpha_2^e\rangle$ of PYRZ at higher frequencies was also obtained, giving a linear relationship with the dipole moment of the solvents.

The PYR ring is a fundamental unit for the formation of PYRZ and the electronic properties of the former should play a central role in determining the electronic polarizability of the latter. For this reason, we decided to carry out the experimental determination of the electronic polarizability of pyrazole in solution. The results are shown in Tables 3 and 4. It is important to note that the dispersion behavior of the dynamic average dipole polarizability of pyrazole, determined in THF solution and using Eqn. (11), as can be seen in Fig. 4, shows that the molecular response is enhanced by the effect of the

Table 4. Results of dipole polarizability of PYR determined from Eqns (11) and (12) in binary solutions

ν (μm^{-1})	$\alpha_2^e(\nu)(10^{-23} \text{ esu})^a$		$\alpha_2^e(\nu)(10^{-23} \text{ esu})$	
	THF	CH ₃ CN	THF	CH ₃ CN
2.294631	0.794	0.815	0.793	0.815
1.966182	0.763	0.791	0.760	0.789
1.831166	0.752	0.783	0.751	0.781
1.696065	0.743	0.776	0.744	0.774
	0.754 ^c			
1.553277	0.734	0.770	0.734	0.769
0.000000	0.695	0.746	0.704	0.751

^a Equation (11) and parameters of Table 3.^b Equation (12) and parameters of Table 3.^c Experiment from molar dynamic refraction in dioxane.²²**Figure 4.** Dispersion curves of the mean dipole polarizability of PYR obtained from Eqn. (11) in solutions of THF and CH₃CN

frequency of the electric field. From this curve, the dynamic average electronic polarizability of PYR at 589.6 nm ($1.696065 \mu\text{m}^{-1}$) is $0.743 \times 10^{-23} \text{ esu}$, which is in excellent agreement with the reported value for pyrazole in dioxane solution ($0.754 \times 10^{-23} \text{ esu}$).²² It is noteworthy that the static electronic average polarizability of two free PYR molecules is about 80% of the static value of PYRZ in the same solvent, and this contribution is maintained in the overall optical regime. This result indicates that, despite the significant differences in molecular symmetry between pyrazole and pyrazabole and therefore different contributions from the axial and orthogonal components of the polarizability tensor due to their connection with the molecular structure, only about 20% of the PYRZ $\langle\alpha\rangle$ value is due to the electronic charge contribution of the two BH₂ bridge units when the pyrazabole molecule is formed. These findings are expected because of the chemical size of the BH₂ units. For PYR, the electric deformability in THF is about 14%, which is much higher than that of PYRZ in THF. When ACN was used (see Table 4), the dynamic polarizability of PYR is increased with respect to THF. For example, the static property for this molecule is 7.34% higher than the value in THF solution (see Fig. 4). Also, a significant decreases in the electric deformability was observed in this case, the corresponding value being about 9.2%. The higher $\langle\alpha\rangle$ of PYR in ACN than in THF indicate that a larger contraction in the electronic density of the pyrazole ring in the polar solvent with respect to that in THF. It is interesting that the values of the dynamic and static polarizability of PYR in CH₃CN solution obtained with Eqns (11) and (12) are very similar, as can be seen in Table 4. In contrast, the optical dispersion of the polarizability of PYR in THF solution showed a marked deviation from a normal dispersion when the Eqn. (12) was applied for the experimental determination of dynamic polarizabilities and it was very difficult to extrapolate the dynamic polarizability to the static value with the Cauchy equation.

Table 5. Geometry parameters for PYR and PYRZ calculated at the HF and B3LYP levels using the 6-31+G(d,p) basis set (x-ray geometry parameters in parentheses^a)

Level	Bond distance Å		Bond angle (°)		Torsion angle (°)	
	PYR	PYRZ	PYR	PYRZ	PYR	PYRZ
HF	a	1.578	γ	103.7		0.0
B3LYP		1.569 (1.554)		104.6 (104.7)	B—N—N—B	0.0
HF	b	1.329	ab	120.5		178.5
B3LYP		1.335 (1.351)		120.1 (120.2)	B—N—C—C	177.9
HF	c	1.342	ac	130.7		0.0
B3LYP		1.319 (1.339)		131.3	N—N—C—C	0.37
HF	d	1.366	bc	112.8		-41.5
B3LYP		1.387 (1.362)		108.8 (108.6)	N—B—N—N	-41.5
HF	e	1.070	cd	106.6		0.0
B3LYP		1.080		109.2	C—N—N—C	0.0
HF	f	1.069	ce	106.2		0.0
B3LYP		1.069		109.0	B—N—N—C	179.0
HF	g	1.079	df	121.8		178.5
B3LYP		1.079		120.1		
HF		1.201		128.3		
B3LYP		1.206 (1.135)		128.0 (127.3)		
HF	h	1.201	ag	109.7		
B3LYP		1.203 (1.111)		109.4 (110.5)		
HF	a'	0.992	ah	109.2		
B3LYP				109.4 (108.2)		
HF	c'	1.304	β	103.9		
B3LYP				104.6 (104.7)		
HF	d'	1.414	a'b	120.1		
B3LYP				118.9		
HF	e'	1.071	bc'	105.2		
B3LYP				104.2		
HF			c'd'	111.5		
B3LYP				111.9		
HF			c'e'	119.4		
B3LYP				119.5		

^a X-ray crystal structure from Ref. 23.

Theoretical calculations. Results of HF/6-31+G(d,p) and B3LYP/6-31+G(d,p) geometry optimization for PYR and PYRZ are reported in Table 5. The labels for the geometric parameters are shown in Fig. 1. A comparison with the geometric structure of PYRZ with the x-ray crystal structure²³ was made, the bond lengths and bond angles being displayed in Table 5 in parentheses. The results show that the structure of the PYR ring does not change significantly when PYRZ is formed. Additionally, good correspondence exists between the HF and B3LYP geometry of PYRZ with the corresponding experimental x-ray geometry.²³

Table 6 shows the total energies, dipole moments μ (debye) and Mulliken atomic populations (MAP) for PYR and PYRZ. The B3LYP/6-311++G(3d,3p) basis set give a μ value of 2.29 D for the PYR molecule, which lies within the range of the experimental μ values in different solvents (2.06–2.33 D). These experimental μ

values confirm that for PYR, the electronic properties are very dependent on the nature of the solvent, and similarly by for PYRZ. In this work, a μ value of 2.66 D is predicted for PYRZ. The MAP of PYR and PYRZ as displayed in Table 6 show that the electronic charges on the atoms of PYR remain almost the same in the PYRZ molecule, indicating that the electronic PYR moiety is not altered in the PYRZ structure. Table 7 displays the α_{ii} components, the average and the anisotropy of the dipole polarizability. These properties were calculated with the HF and B3LYP methods and the 6-31+G(d,p) and 6-311++G(3d,3p) basis sets. For PYR, calculations were additionally performed for the polarizability with the Sadlej basis sets. The results indicate that the values obtained with the Sadlej basis set are similar to those obtained with the 6-311++G(3d,3p) basis. For PYR and PYRZ our best estimated values of the average polarizability $\langle\alpha\rangle$ are 0.727×10^{-23} and 1.877×10^{-23} esu,

Table 6. Total energies E_t , dipole moments μ and Mulliken's atomic charges of PYR and PYRZ at the HF and B3LYP levels using the (A) 6-31+G(d,p) and (B) 6-311++G(3d,3p) basis sets

	PYR			PYRZ		
	HF/A	B3LYP/A	B3LYP/B	HF/A	B3LYP/A	B3LYP/B
E_t (hartree)	-224.81142	-226.21900	-226.27502	-500.27021	-503.47381	-503.59186
μ (D)	2.49	2.41	2.29 (2.06–2.33) ^a	2.91	2.71	2.66
q_{N1}	-0.29	-0.21	-0.26	-0.22	-0.14	-0.22
$q_{N1'}$	-0.22	-0.20	-0.61	—	—	—
q_B	—	—	—	0.63	0.43	0.15
q_{C1}	-0.10	-0.20	0.10	-0.24	-0.32	-0.01
$q_{C1'}$	-0.12	-0.18	-0.02	—	—	—
q_{C2}	-0.16	0.04	0.31	-0.06	0.15	0.32

^a Experimental values in different solvents.²⁴

respectively. The comparison of these values with respect to our experimental values with the Singer and Garito method gives for PYR a variation of 6.0% (THF) and -1.2% (ACN), whereas for PYRZ the corresponding variations are 4.7% (cyclohexane), 8.5% (ACN) and 2.8% (THF), respectively.

The results from TDHF calculations with the 6-31+G(d,p), 6-311++G(3d,3p) and Sadlej basis sets of the dynamic dipole polarizability of pyrazole are shown in Table 8. This table also contains the *A* and *B* coefficients of the Cauchy curves and the corresponding correlation coefficients. These dynamic polarizabilities of PYR follow a regular Cauchy dispersion that is similar to those shown in Figs 4 and 5. However, for higher frequencies, TDHF calculations in the gas phase do not reproduce the experimental tendencies of the dynamic polarizabilities.

CONCLUSIONS

The results showed that the experimental refraction technique of Singer and Garito and of Proutière and co-workers at the infinite dilution limit were appropriate for describing the dispersion behavior of the dynamic polarizability of pyrazabole and pyrazole in solution in

the off-resonance region. It was shown that the pyrazabole is a highly polarizable compound in solution and its dynamic polarizability is dependent of the dielectric nature and the polarity of the solvents. The static and dynamic electronic polarizability are not affected in cyclohexane and THF solvents, whereas an important variation in this property and in the electric deformability was observed in a dipolar and non-hydrogen bond donor solvent such as ACN. It was found that at higher frequencies, there is a linear relationship between the dynamic $\langle\alpha\rangle$ of PYRZ and the dipole moments μ of the three solvents employed, whereas in the region of lower frequencies the polarizability of PYRZ is higher in a solvent with lower μ and decreases for a solvent with the higher μ . These differences in the behavior of $\langle\alpha\rangle$ in terms of the solvent properties are being studied carefully, but a large amount of data is required to establish the underlying relationships between the solvent parameters and the electronic properties of PYRZ.

From the comparative study of the electronic polarizability of the studied compounds in the static and dynamic regimes, we conclude that the properties of the pyrazole ring have an important influence on the overall α value of the pyrazabole molecule, whereas the contribution of the polarizability and electric deformability of the BH₂ bridge units is very low.

Table 7. Static dipole polarizability components (α_{aa} , α_{bb} , α_{cc}), average polarizability (α_{ave}) and anisotropy of polarizability ($\Delta\alpha$) (10^{-23} esu) of PYR and PYRZ

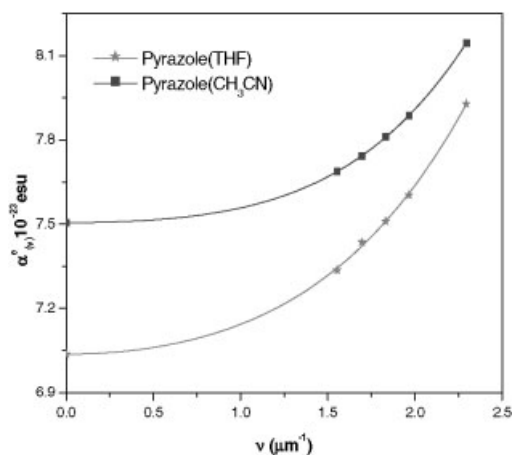
		PYR			PYRZ	
		6-31+G(d,p)	6-311++G(3d,3p)	Sadlej	6-31+G(d,p)	6-311++G(3d,3p)
HF	α_{aa}	0.716	0.758	0.765	1.988	2.093
	α_{bb}	0.747	0.787	0.795	1.736	1.806
	α_{cc}	0.444	0.490	0.490	1.235	1.300
	α_{ave}	0.636	0.678	0.684	1.653	1.733
	$\Delta\alpha$	0.289	0.284	0.291	0.664	0.695
B3LYP	α_{aa}	0.802	0.836	0.851	2.216	2.304
	α_{bb}	0.797	0.837	0.852	1.888	1.956
	α_{cc}	0.467	0.507	0.508	1.310	1.370
	α_{ave}	0.689	0.727	0.737	1.805	1.877
	$\Delta\alpha$	0.333	0.329	0.344	0.795	0.818

Table 8. Time-dependent Hartree–Fock (TDHF) average dipole polarizability $\alpha(\nu)$ (10^{-23} esu) of PYR

ν (μm^{-1})	6-31+G(d,p)	6-311++G(3d,3p)	Sadlej
2.294631	0.672	0.713	0.723
1.966182	0.662	0.702	0.712
1.831166	0.658	0.698	0.708
1.696065	0.655	0.695	0.704
1.553277	0.652	0.692	0.701
0.000000	0.636	0.675	0.684
$\alpha(0)^a$	0.636	0.675	0.684
A	0.06292	0.06524	0.06763
B	0.00134	0.00138	0.00144
R^{2b}	1.0	1.0	1.0

^a Results from the fitting to a Cauchy dispersion curve [$\alpha(\nu) = \alpha(0) + A\nu^2 + B\nu^4$].

^b Multiple correlation coefficient.

**Figure 5.** Dispersion curves of the mean dipole polarizability of PYR obtained from Eqn. (12) in solutions of THF and CH₃CN

The measured static $\langle\alpha\rangle$ values for PYR were 0.695 (THF) and 0.746 esu (ACN) and for PYRZ were 1.792 (cyclohexane), 1.826 (THF) and 1.730×10^{-23} esu (ACN). The B3LYP/6-311++G(3d,3p) theoretical results for the polarizability of PYR (0.727×10^{-23} esu) and for PYRZ (1.877×10^{-23} esu) are comparable to the experimental values. The differences between the theoretical and experimental values lie in the range 2.8–4.7%. These variations are mainly due to the solvent effects observed on the dipole polarizability of the molecules studied in solution.

The results from TDHF of the dynamic dipole polarizability of pyrazole follow a Cauchy curve dispersion with correlation coefficient of 1.0.

Acknowledgements

The authors thanks CONICIT of Venezuela (Grant No. S1-95001617), CONICIT/CONIPET (No. 58 97003734), CONICIT (PG No. G-97000593) and CONDES/LUZ for partial financial support.

REFERENCES

- (a) Trofimenko S. *J. Am. Chem. Soc.* 1967; **89**: 3165–3177; (b) Trofimenko S. *Prog. Inorg. Chem.* 1986; **34**: 115–210.
- (a) Trofimenko S. *Chem. Rev.* 1993; **93**: 943–980; (b) Kitajima N. *Prog. Inorg. Chem.* 1995; **43**: 419–531.
- (a) Hernandez FE, Marcano AO, Alvarado Y, Biondi A, Mailotte H. *Opt. Commun.* 1998; **152**: 77–82; (b) Campo JA, Cano M, Heras JV, Lopez-Garabito C, Pinilla E, Torres R, Rojo G, Agullo-Lopez F. *J. Mater. Chem.* 1999; **9**: 899–907; (c) McCleverty JA. *Polyhedron* 1989; **8**: 1669–1674.
- (a) Kresinski RA. *J. Chem. Soc., Dalton Trans.* 1999; 401–405; (b) Niedenzu K, Niedenzu PM. *Inorg. Chem.* 1984; **23**: 3713–3716.
- Dabrowski M, Serwatowski J, Sporzynski A. *J. Chem. Eng. Data* 1997; **42**: 1111–1115.
- (a) Jakle F, Priermeier T, Wagner M. *Organometallics* 1996; **15**: 2033–2040; (b) Herdtweck E, Jakle F, Oromolla G, Spiegler M, Wagner M, Zanello P. *Organometallics* 1996; **15**: 5524–5535.
- Barbera J, Giménez Serrano JL. *Chem. Mater.* 2000; **12**: 481–489.
- Soscún H, Alvarado Y, Hernández J, Hernandez P, Atencio R, Hinchliffe A. *J. Phys. Org. Chem.* 2001; **14**: 709–715.
- (a) Buckingham AD. *Adv. Chem. Phys.* 1967; **12**: 107–142; (b) Hinchliffe A, Soscún-Machado HJ. *Int. J. Mol. Sci.* 2000; **1**: 39–48; (c) Miller CK, Ward, JF. *Phys. Rev. A* 1977; **16**: 1179–1185; (d) Hinchliffe A, Munn R. *Molecular Electromagnetism*. Wiley: Chichester, 1985.
- (a) Singer KD, Garito AF. *J. Chem. Phys.* 1981; **75**: 3572–3580; (b) Hohm U, Goebel D, Grimme S. *Chem. Phys. Lett.* 1997; **272**: 328–334; (c) Gussoni M, Rui M, Zerbi G. *J. Mol. Struct.* 1998; **447**: 163–216.
- Heraïl M, Le Guennec M, Le Goff D, Proutière A. *J. Mol. Struct.* 1996; **380**: 171–194.
- Alvarado Y, Cubillán N, Labarca PH, Karam A, Arrieta F, Castellano O, Soscún H. *J. Phys. Org. Chem.* 2002; **15**: 154–164.
- Böttcher, CJF. *Theory of Dielectric Polarization*, Vol. 1. Elsevier: Amsterdam, 1973.
- (a) Parr RG, Yang W. *Density-functional Theory of Atoms and Molecules*. Oxford University Press: Oxford, 1989; (b) Becke AD. *Phys. Rev. A* 1988; **38**: 3098–3100; (c) Lee C, Yang W, Parr RG. *Phys. Rev. B* 1988; **37**: 785–789; (d) Becke AD. *J. Chem. Phys.* 1993; **98**: 5648–5652.
- Clark T, Chandrasekhar J, Spitznagel GW, Schleyer PvR. *J. Comput. Chem.* 1983; **4**: 294–301.
- Dykstra CE, Jasien PG. *Chem. Phys. Lett.* 1984; **109**: 388–393.
- Frisch MJ, Pople JA, Binkley JS. *J. Chem. Phys.* 1984; **80**: 3265–3269, and references cited therein.
- (a) Sadlej AJ. *Collect. Czech. Chem. Commun.* 1988; **53**: 1995–2010; (b) Sadlej AJ, Urban M. *J. Mol. Struct. (THEOCHEM)* 1991; **234**: 147–160; (c) Sadlej AJ. *Theor. Chim. Acta* 1991; **79**: 123–140; (d) Sadlej AJ. *Theor. Chim. Acta* 1991; **81**: 45–63; (e) Sadlej AJ. *Theor. Chim. Acta* 1991; **81**: 339–354.
- Karna SP, Dupuis M. *J. Comput. Chem.* 1991; **12**: 487–504.
- Frisch MJ, Trucks GW, Schlegel HB, Scuseria GE, Robb MA, Cheeseman JR, Zakrzewski VG, Montgomery JA Jr., Stratmann RE, Burant JC, Dapprich S, Millam JM, Daniels AD, Kudin KN, Strain MC, Farkas O, Tomasi J, Barone V, Cossi M, Cammi R, Mennucci B, Pomelli C, Adamo C, Clifford S, Ochterski J, Petersson GA, Ayala PY, Cui Q, Morokuma K, Malick DK, Rabuck AD, Raghavachari K, Foresman JB, Cioslowski J, Ortiz JV, Baboul AG, Stefanov BB, Liu G, Liashenko A, Piskorz P, Komaromi I, Gomperts R, Martin RL, Fox DJ, Keith T, Al-Laham MA, Peng CY, Nanayakkara A, Gonzalez C, Challacombe M, Gill PMW, Johnson B, Chen W, Wong MW, Andres JL, Gonzalez C, Head-Gordon M, Replogle ES, Pople JA. *Gaussian 98*, Revision A.7. Gaussian: Pittsburgh, PA, 1998.
- Cheng LP, Tam W, Stevenson SH, Meredith GR, Rikken G, Marder SR. *J. Phys. Chem.* 1991; **95**: 10631–10643.
- Calderbank KE, Calvert RL, Lukins PB, Ritchie GLD. *Aust. J. Chem.* 1981; **34**: 1835–1844.
- Hanecker E, Hodgkins TG, Niedenzu K, Nöth H. *Inorg. Chem.* 1985; **24**: 459–462.
- Aksamentova TN, Krivoruchka IG, Elokina VN, Vokin VA, Lopyrev VA, Turchaninov VK. *Russ. Chem. Bull.* 1999; **48**: 2176–2177.